

## A DERIVED PHYSICALLY EXPRESSIVE CIRCUIT MODEL FOR ELECTRICALLY SMALL RADIATING STRUCTURES

Lap Kun Yeung\* and Ke-Li Wu

Department of Electronic Engineering, The Chinese University of Hong Kong, Shatin NT, Hong Kong, China

**Abstract**—Recently, a new radiation model for the partial element equivalent circuit (PEEC) technique has been proposed. This model makes use of the concept of generalized complex inductance to account for the radiation effect and preserve the (quasi-)static condition for the capacitance. Therefore, PEEC models with the radiation effect included consists of real-valued capacitors but complex-valued inductors. In this paper, a method for deriving a concise and physically intuitive equivalent circuit from such a radiating PEEC model is presented. The method is based on the  $Y$ -to- $\Delta$  transformation to eliminate all “unimportant” internal circuit nodes and results in an equivalent circuit with only a few nodes left. The equivalent circuit for a short electric dipole is first derived analytically to offer a simple explanation to the basic principles. The proposed method is then applied to several practical and electrically small antennas for more detailed demonstrations. Numerical results obtained from these examples suggest that a physically intuitive circuit model can potentially be derived for arbitrary radiating multi-conductor structures, showing the method is useful for analysis and design of modern integrated and electrically small antennas.

### 1. INTRODUCTION

The number of radio systems in handheld wireless devices has been growing rapidly during the last several years from typically two systems to almost ten, including FM, GSM, 3G, WLAN, Bluetooth, and etc.. On the other hand, the major trend of these devices today is towards smaller size and longer battery life. This, indeed, posts a serious

---

*Received 15 March 2013, Accepted 22 May 2013, Scheduled 29 May 2013*

\* Corresponding author: Lap Kun Yeung (lkyeung@msn.com).

challenge to antenna designers because there is a fundamental limit on how small an antenna can be but without scarifying too much of its performance. For such modern wireless devices, instead of traditional monopole-like configurations, small-size integrated antennas of better efficiency and more complex in shape are often required. These antennas usually operate at multiple frequency bands and have strict performance requirements, and thus need more sophisticated tools to design.

Nowadays, a variety of numerical techniques exists for modeling electromagnetic (EM) phenomena, such as method of moments (MoM), finite-difference time-domain (FDTD) method, and finite-element method (FEM). Among all existing techniques, the partial element equivalent circuit (PEEC) technique [1] has been widely used for modeling of different electromagnetic-related issues [2–4], including electro-magnetic compatibility (EMC), electromagnetic interference (EMI), as well as signal integrity (SI) for high-speed electronic circuits. The major reason for its attractiveness is that it can convert a physical layout to a mesh-dependent lumped-element circuit network, which can easily be solved by conventional circuit solvers. Over a few decades of development, the PEEC technique has evolved to a complete numerical algorithm in solving more and more complex problems and found itself many new applications. In fact, the combined circuit and electromagnetic approach makes this technique also a suitable tool for antenna design and verification. As it can offer a direct integration to other circuit models, a complete antenna system can be analyzed in a straightforward manner.

Nevertheless, as far as we know, there are only few PEEC-based models that can handle the radiation effect. All existing ones involve the use of time-retarded control sources [5, 6], which may not be physically intuitive. Recently, a radiation model for the PEEC technique has been proposed [7]. This model makes use of the concept of generalized complex inductance to account for the radiation effect and the resulting equivalent circuit can be used as a starting point to extract all essential information on the radiation characteristics of the structure being investigated. In this paper, a method for deriving a concise and physically intuitive equivalent circuit from such a radiating PEEC model is proposed. The concise circuit obtained from this method should provide significant physical insights to the structure being modeled. A simple example, namely, a short thin metal strip (electric dipole) is first used to explain the basic concept. Then, several practical radiating structures are considered to show the potential of this method for analysis and design of integrated antennas.

## 2. THEORY

### 2.1. Radiation Model for PEEC

A new radiation model for PEEC has been proposed recently. From the derivation given in [7] for the free-space case, the coefficient of potential between two capacitive meshes  $i$  and  $n$  is defined as

$$pp_{i,n} = \frac{1}{a_i a_n} \iint \frac{e^{-jkR}}{4\pi\epsilon_0 R} ds'_n ds_i, \quad (1)$$

where  $a_i$  and  $a_n$  are the areas of the two corresponding meshes. Under the (quasi-)static assumption, where  $kR \ll 1$ , one may assume  $e^{-jkR} \approx 1$  and invert the coefficient of potential matrix to obtain the short-circuited capacitances  $c_{i,n}$ 's. In order to preserve this capacitance definition in a full-wave analysis, the frequency dependent portion of (1) should be extracted out and incorporated only into the inductance matrix. Mathematically, this is done by first separating the integral in (1) into two parts as

$$pp_{i,n} = pp_{i,n}^0 + pp_{i,n}^f = \frac{1}{a_i a_n} \iint \frac{1}{4\pi\epsilon_0 R} ds'_n ds_i + \frac{1}{a_i a_n} \iint \frac{e^{-jkR} - 1}{4\pi\epsilon_0 R} ds'_n ds_i. \quad (2)$$

The first integral in (2) is the conventional (quasi-)static coefficient of potential from which the short-circuited capacitance matrix can be obtained. On the other hand, the frequency dependent second integral is included only in the inductance matrix calculation, in which, the generalized mutual inductance between two inductive meshes  $l$  and  $m$  is defined in [7] as

$$L_{l,m} = \bar{L}_{l,m} + \frac{pp_{l^+,n_1}^f}{\omega^2} - \frac{pp_{l^-,n_1}^f}{\omega^2} - \frac{pp_{l^+,n_2}^f}{\omega^2} + \frac{pp_{l^-,n_2}^f}{\omega^2}, \quad (3)$$

where  $n_1$ ,  $n_2$  and  $l^+$ ,  $l^-$  are the capacitive meshes connecting to the two ends of inductive mesh  $m$  and  $l$  respectively. The original self- ( $l = m$ ) or mutual inductance term of

$$\bar{L}_{l,m} = \frac{1}{w_l w_m} \iint \frac{\mu_0 e^{-jkR}}{4\pi R} ds'_m ds_l, \quad (4)$$

where  $w_l$  and  $w_m$  are the widths of the corresponding meshes, is generalized by "absorbing" the second integral in (2). The significance of introducing such a generalized inductance is that it can correctly account for the radiation effect and, at the same time, preserve the (quasi-) static condition for the capacitance matrix.

Let's consider a simple short thin metal strip of length  $l$  and width  $w$  as shown in Fig. 1. The dipole is divided into one inductive (solid) and two capacitive (dotted) meshes, resulting in an equivalent circuit as shown also in Fig. 1. It can be derived that the generalized inductance in this case is given by

$$L = \frac{\mu_0}{4\pi w^2} \iint \frac{1}{R} ds' ds - \frac{\mu_0 l}{4\pi} - j \left( \frac{\mu_0 k l^2}{6\pi} \right). \quad (5)$$

The real part of  $j\omega L$  can be interpreted as a frequency dependent resistance with the value of

$$R = 80\pi^2 \left( \frac{l}{\lambda} \right)^2, \quad (6)$$

which is exactly equal to the well-known radiation resistance of a short dipole given in the classical antenna theory [8]. The imaginary part of generalized inductance in fact represents the radiation loss of the strip. In order to have a better picture of the radiation model, a

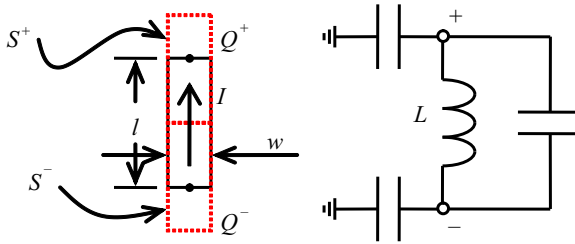


**Figure 1.** Short metal strip and its two-mesh (capacitive) PEEC model.

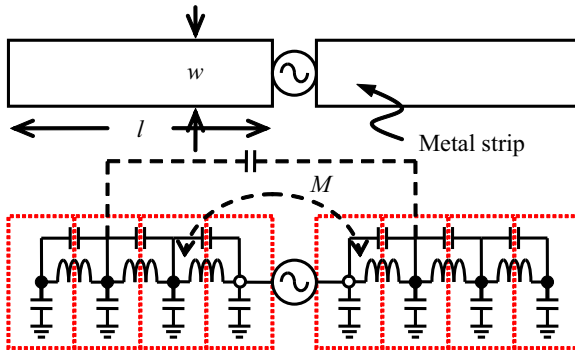


**Figure 2.** Center-fed thin-strip dipole and its PEEC model.

full-fledged antenna example is shown in Fig. 2. Here, a thin-strip center-fed dipole and its eight-mesh (capacitive) PEEC model with complex-valued inductors are depicted. Notice that not all mutual components are shown in the figure for clarity. This example clearly shows that the PEEC model, in general, can be quite complicated.

### 2.2. Model Order Reduction

For a typical PEEC analysis, the resulting equivalent circuit is mesh dependent and usually contains a large number of elements. Therefore, in general, it is difficult to obtain any physical insights by directly examining the circuit itself. This fact is well illustrated in the center-fed dipole example given above. In order to obtain a more concise and physically intuitive circuit model, the model order reduction (MOR) technique [9, 10] can be applied. In this work, the one introduced in [11] is used. This technique is based on the principle of  $Y$ -to- $\Delta$  transformation to eliminate all “unimportant” internal circuit nodes. The reduced circuit thus contains only a few nodes and is physically intuitive. Fig. 3 demonstrates the node elimination principle. Here, node 0 is being eliminated and new admittances between each pair of remaining nodes can be calculated by

$$y_{ij} = \frac{y_i y_j}{y_t} \quad \text{with} \quad y_t = y_1 + y_2 + y_3 + y_4, \tag{7}$$

for  $i \neq j$  and  $i, j = 1, \dots, 4$ . Specifically, as the PEEC model has its branches consist of either a single capacitor or a parallel LC-tank, the  $i$ -th branch admittance takes the form of

$$y_i = j\omega C_i + \frac{1}{j\omega L_i}. \tag{8}$$

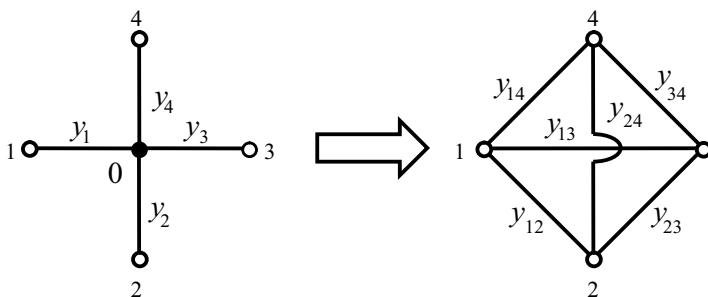


**Figure 3.** Node elimination principle.

Substituting (8) into (7), the new admittance between node  $i$  and node  $j$  can be expressed as

$$y_{ij} = j\omega C_{ij} + \frac{1}{j\omega L_{ij}}, \quad (9)$$

with

$$C_{ij} = \frac{\overbrace{C_i C_j}^{\bar{C}_{ij}}}{C_t} + \frac{\alpha L_t}{1 - \omega^2 L_t C_t} \quad \text{and} \quad L_{ij} = \frac{L_i L_j}{L_t}, \quad (10)$$

where  $a = C_i/L_j + C_j/L_i - \bar{C}_{ij}/L_t - C_t/L_i j$ , and  $L_t$  and  $C_t$  are the total inductance and capacitance connecting to the node that is being deleted. Two important points can be observed here. Firstly, the capacitance  $C_{ij}$  is mixed with the inductance  $L_t$  after the  $Y$ -to- $\Delta$  transformation. In other words, the capacitive components of the simplified circuit are generally complex in value, which implies that there is radiation loss (or gain) associated with each of them. For example, the new capacitance  $C_{ij}$  in (10) is a function of  $L_t$  and  $\alpha$ . As these two terms are complex in value,  $C_{ij}$  is also complex in value with its imaginary part equivalent to a conductance (after multiplying to  $j\omega$ ). Secondly, the term  $\omega^2 L_t C_t$  can be used as a criterion to determine how concise the final simplified circuit model should be. For an internal node that has the condition of  $\omega^2 L_t C_t \ll 1$ , its coupling to all other connecting nodes is small. Thus, this node can be considered “unimportant” and can be eliminated. In practice, a cutoff value  $\delta$  can be preset such that all the internal nodes satisfying the condition of  $\omega^2 L_t C_t < \delta$  should be removed. And hence, the complexity of the resulting simplified circuit depends on how small this value is.

To illustrate this MOR concept, let's consider again the short metal strip example discussed earlier under the three-mesh (capacitive) configuration. As shown in Fig. 4, the PEEC model consists of two (complex) inductors and six capacitors. Using (3) and (4), the expressions for the two generalized self-inductances are obtained as

$$L_a = \frac{\mu_0}{4\pi w^2} \iint \frac{1}{R} ds' ds - \frac{\mu_0 l_a}{4\pi} - j \left( \frac{\mu_0 k l_a^2}{6\pi} \right), \quad (11a)$$

$$L_b = \frac{\mu_0}{4\pi w^2} \iint \frac{1}{R} ds' ds - \frac{\mu_0 l_b}{4\pi} - j \left( \frac{\mu_0 k l_b^2}{6\pi} \right), \quad (11b)$$

where  $l_a + l_b = l$  and that for the mutual inductance is

$$M = \frac{\mu_0}{4\pi w^2} \iint \frac{1}{R} ds' ds - j \left( \frac{\mu_0 k l_a l_b}{6\pi} \right). \quad (12)$$

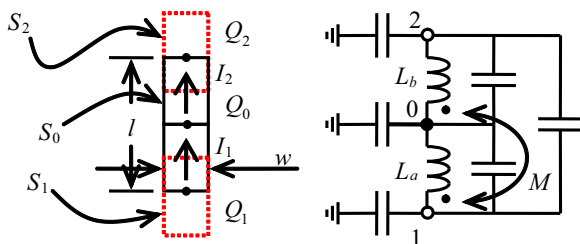


**Figure 4.** Three-mesh (capacitive) PEEC model of a short metal strip.

The equivalent circuit shown in Fig. 4 contains one internal node, namely, node 0. To simplify this circuit, this internal node can be eliminated. The first step is to convert the pair of mutually coupled inductors into a set of directly connected inductors as depicted in Fig. 5. Then, node 0 is eliminated by applying the  $Y$ -to- $\Delta$  transformation, resulting in a  $\pi$ -network consisting of admittances  $Y_1$ ,  $Y_2$ , and  $Y_{12}$ . Using (9) and (10), it can be shown that

$$Y_{12} = \frac{L_t}{j\omega L_1 L_2} + j\omega \frac{C_1 C_2}{C_t} + \frac{j\omega}{1 - \omega^2 L_t C_t} \left( C_1 k_2 + C_2 k_1 - \frac{C_1 C_2}{C_t} - C_t k_1 k_2 \right), \quad (13)$$

with  $k_1 = L_t/L_1$  and  $k_2 = L_t/L_2$ . The overall inductance across node 1 and node 2 is then equal to  $L_{12}$  in parallel with the inductive part of  $Y_{12}$ , which is

$$\left( \frac{1}{L_{12}} + \frac{L_t}{L_1 L_2} \right)^{-1} = L_a + L_b + 2M. \quad (14)$$

The real part of  $j\omega(L_a + L_b + 2M)$ , which represents the radiation loss, is once again equal to (6) with the use of (11) and (12). This

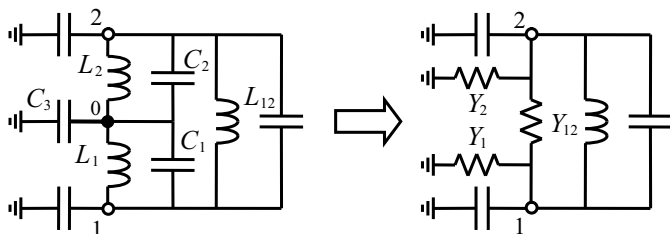


**Figure 5.** Simplification of the PEEC model.

result suggests that the once mesh-dependent circuit (Fig. 4) can be simplified to a more concise circuit (Fig. 1), which contains all the essences of the metal strip being modeled.

Notice that, the criterion of  $\omega^2 L_t C_t < \delta$  is assumed valid for node 0 in the above simplification exercise. Therefore, the three-mesh PEEC model is reduced to its simplest form, which contains only two external nodes. Obviously, if  $\delta$  is set to a very small value such that the condition cannot be satisfied, node 0 will not be removed and the PEEC model will remain the same. In fact, this illustrates how the parameter  $\delta$  can be used to determine the conciseness of the final circuit.

### 3. NUMERICALLY RESULTS

#### 3.1. Small Thin-strip Dipoles

An antenna is usually considered to be electrically small if it satisfies the inequality of  $ka < 0.5$ , where  $k$  is the free-space propagation constant and  $a$  is the radius of the smallest sphere that can completely

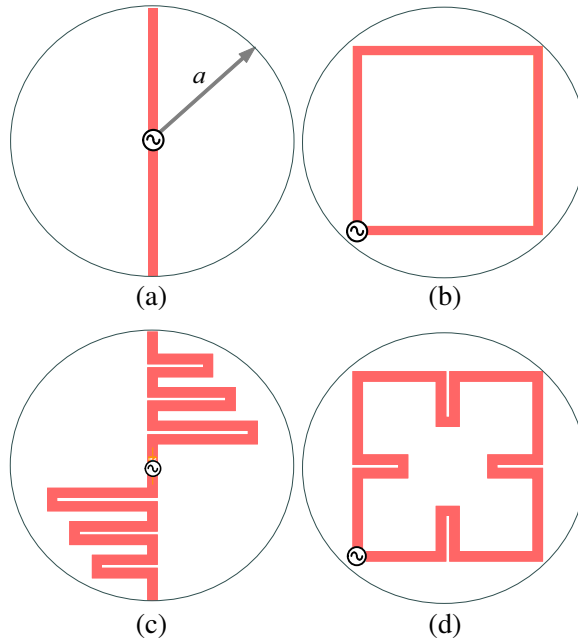


**Figure 6.** Various small antennas including (a) straight and (c) meandered dipoles, (b) square and (d) meandered loops.

encloses the antenna [8]. With this definition, two electrically small thin-strip dipoles, namely, a straight dipole and a meandered dipole (Fig. 6) are investigated here with  $ka = 0.5$  at 4 GHz. Assuming there is no conductor loss, it is expected that the meandered dipole should have a smaller radiation quality ( $Q$ ) factor when comparing to the straight one. However, this fact cannot be seen by directly looking at their PEEC models, which contain a large number of elements. Specifically, the model for the straight dipole contains 136 capacitors and 14 mutually coupled inductors (corresponding to 16 capacitive meshes) whereas the one for the meandered dipole contains 1953 capacitors and 60 mutually coupled inductors (corresponding to 62 capacitive meshes). On the other hand, their concise circuits derived by using the MOR technique discussed above can readily provide information on the  $Q$  factor. In both cases, the original PEEC models are simplified (with a large  $\delta$ ) to the (a) circuit shown in Fig. 7 with the corresponding component values listed in Table 1 and Table 2, respectively.

**Table 1.** Component values for the straight dipole.

Freq. (GHz)	$C_a$ (F)	$C_b$ (F)
1	$1.45 \times 10^{-14} - j3.62 \times 10^{-18}$	$7.31 \times 10^{-14} - j2.30 \times 10^{-21}$
2	$1.48 \times 10^{-14} - j3.01 \times 10^{-17}$	$7.37 \times 10^{-14} - j7.51 \times 10^{-20}$
3	$1.55 \times 10^{-14} - j1.08 \times 10^{-16}$	$7.47 \times 10^{-14} - j5.96 \times 10^{-19}$
4	$1.65 \times 10^{-14} - j2.81 \times 10^{-16}$	$7.62 \times 10^{-14} - j2.67 \times 10^{-18}$

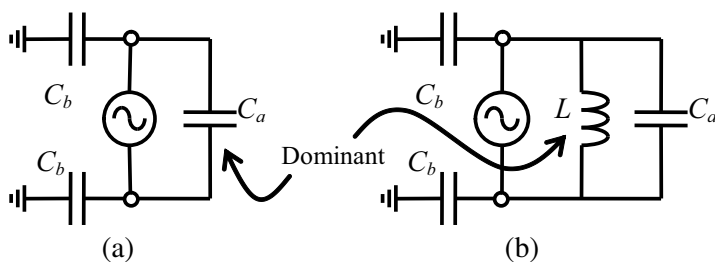


**Figure 7.** Electrically small antenna circuit models: (a) electric type and (b) magnetic type.

By looking at these concise circuits, it is clear that the two antennas are both electric-type within the operating frequency band of interest ( $< 4$  GHz) because both of them can be modeled by a circuit

**Table 2.** Component values for the meandered dipole.

Freq. (GHz)	$C_a$ (F)	$C_b$ (F)
1	$4.50 \times 10^{-14} - j1.95 \times 10^{-17}$	$1.37 \times 10^{-13} - j7.79 \times 10^{-21}$
2	$5.09 \times 10^{-14} - j1.91 \times 10^{-16}$	$1.44 \times 10^{-13} - j2.97 \times 10^{-19}$
3	$6.53 \times 10^{-14} - j9.76 \times 10^{-16}$	$1.59 \times 10^{-13} - j3.12 \times 10^{-18}$
4	$1.08 \times 10^{-13} - j5.26 \times 10^{-15}$	$1.92 \times 10^{-13} - j2.37 \times 10^{-17}$

dominated by only capacitors. Another interesting fact is that these complex-valued capacitors have their imaginary values increase with the operating frequency. In essence, the imaginary part of such a capacitor represents its loss from radiation. When looking into the excitation port, the (left) circuit in Fig. 7 can be further simplified to contain just a single capacitor of value  $C = C_a + C_b/2$ . Its quality factor is approximately the radiation  $Q$  factor of the antenna. Fig. 8 shows the excitation port admittances and approximated  $Q$  factors (triangle markers) for the two antennas at different operating frequencies. It can be seen from the figure that the radiation conductance of the meandered dipole is generally larger and increases rapidly when  $ka$  approaching 0.5. To verify the accuracy of these derived concise circuit models, results (solid lines) obtained from a commercial full-wave electromagnetic solver are also shown and they agree well with each other.

### 3.2. Small Thin-strip Dipoles

An electrically small loop is a magnetic-type antenna because its stored reactive energy is mainly inductive. In this sense, the derived concise (right) circuit given in Fig. 7 should be dominated by the inductor. An electrically small thin-strip square loop and a meandered loop are investigated with again  $ka = 0.5$  at 4 GHz. Using the MOR technique discussed above, the component values for the two loops are derived and listed in Table 3 and Table 4, respectively. Notice that, from the perspective of the excitation port, the three capacitors can be combined into a single one and the overall capacitance is again given by the formula  $C = C_a + C_b/2$ . The calculated admittances and approximated radiation  $Q$  factors are plotted also in Fig. 8. The results from these concise circuit models agree well with the full-wave solutions. Comparing with their corresponding PEEC models, a significant simplification has been achieved for both cases. Specifically, the PEEC model for the square loop contains 276 capacitors and 22

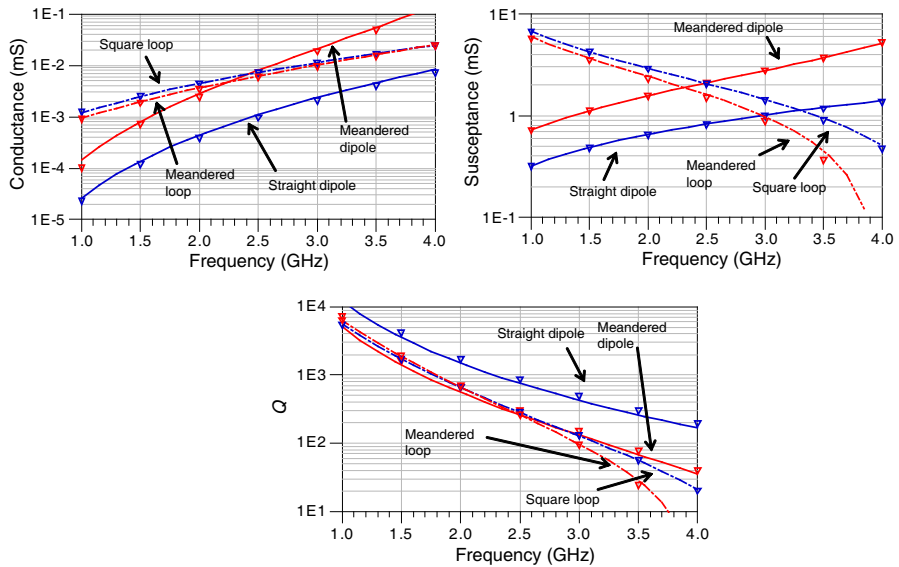


**Figure 8.** Excitation port admittances and approximated radiation  $Q$  factors for various electrically small antennas. Solid curves are results from a commercial full-wave MoM solver and triangular markers are results from the proposal method.

**Table 3.** Component values for the square loop.

Freq. (GHz)	$C = C_a + C_b/2$ (F)	$L$ (F)
1	$4.48 \times 10^{-14} - j3.39 \times 10^{-17}$	$2.32 \times 10^{-08} - j3.42 \times 10^{-12}$
2	$4.54 \times 10^{-14} - j9.74 \times 10^{-17}$	$2.33 \times 10^{-08} - j2.12 \times 10^{-11}$
3	$4.66 \times 10^{-14} - j2.31 \times 10^{-16}$	$2.34 \times 10^{-08} - j6.72 \times 10^{-11}$
4	$4.85 \times 10^{-14} - j5.01 \times 10^{-16}$	$2.36 \times 10^{-08} - j1.54 \times 10^{-10}$

mutually coupled inductors (corresponding to 23 capacitive meshes) whereas the one for the meandered loop contains 1128 capacitors and 46 mutually coupled inductors (corresponding to 47 capacitive meshes). It is interesting to see that, unlike the dipole case, there is no significant improvement on the  $Q$  factor by meandering of the loop.

### 3.3. Radiation Efficiency

When substrate loss and conductor loss are included in the PEEC analysis, the radiation efficiency of these antennas can also be

quickly calculated from their associated concise circuit models. Generally speaking, such losses can be modeled by having finite-valued conductivity (conductor loss) and complex-valued permittivity (substrate loss), which thus lead to an extra resistance term to the inductance and an extra conductance term to the capacitance.

**Table 4.** Component values for the meandered loop.

Freq. (GHz)	$C = C_a + C_b/2$ (F)	$L$ (F)
1	$5.52 \times 10^{-14} - j3.36 \times 10^{-17}$	$2.65 \times 10^{-08} - j3.06 \times 10^{-12}$
2	$5.65 \times 10^{-14} - j1.05 \times 10^{-16}$	$2.66 \times 10^{-08} - j1.83 \times 10^{-11}$
3	$5.89 \times 10^{-14} - j2.73 \times 10^{-16}$	$2.68 \times 10^{-08} - j5.75 \times 10^{-11}$
4	$6.28 \times 10^{-14} - j6.61 \times 10^{-16}$	$2.69 \times 10^{-08} - j1.32 \times 10^{-10}$

**Table 5.** Component values for the lossy straight dipole.

Freq. (GHz)	$C_a$ (F)	$C_b$ (F)
1	$1.45 \times 10^{-14} - j4.69 \times 10^{-18}$	$7.31 \times 10^{-14} - j3.78 \times 10^{-18}$
2	$1.48 \times 10^{-14} - j3.24 \times 10^{-17}$	$7.37 \times 10^{-14} - j7.82 \times 10^{-18}$
3	$1.55 \times 10^{-14} - j1.12 \times 10^{-16}$	$7.47 \times 10^{-14} - j1.27 \times 10^{-17}$
4	$1.65 \times 10^{-14} - j2.87 \times 10^{-16}$	$7.62 \times 10^{-14} - j1.97 \times 10^{-17}$

**Table 6.** Component values for the lossy meandered dipole.

Freq. (GHz)	$C_a$ (F)	$C_b$ (F)
1	$4.50 \times 10^{-14} - j5.82 \times 10^{-17}$	$1.37 \times 10^{-13} - j6.40 \times 10^{-17}$
2	$5.09 \times 10^{-14} - j2.94 \times 10^{-16}$	$1.44 \times 10^{-13} - j1.51 \times 10^{-16}$
3	$6.53 \times 10^{-14} - j1.24 \times 10^{-15}$	$1.59 \times 10^{-13} - j3.11 \times 10^{-16}$
4	$1.08 \times 10^{-13} - j6.27 \times 10^{-15}$	$1.92 \times 10^{-13} - j7.32 \times 10^{-16}$

**Table 7.** Component values for the lossy square loop.

Freq. (GHz)	$C = C_a + C_b/2$ (F)	$L$ (H)
1	$4.48 \times 10^{-14} - j2.94 \times 10^{-17}$	$2.32 \times 10^{-08} - j3.05 \times 10^{-10}$
2	$4.54 \times 10^{-14} - j1.00 \times 10^{-16}$	$2.33 \times 10^{-08} - j1.72 \times 10^{-10}$
3	$4.66 \times 10^{-14} - j2.39 \times 10^{-16}$	$2.34 \times 10^{-08} - j1.68 \times 10^{-10}$
4	$4.85 \times 10^{-14} - j5.15 \times 10^{-16}$	$2.36 \times 10^{-08} - j2.30 \times 10^{-10}$

**Table 8.** Component values for the lossy meandered loop.

Freq. (GHz)	$C = C_a + C_b/2$ (F)	$L$ (H)
1	$5.52 \times 10^{-14} - j3.50 \times 10^{-17}$	$2.65 \times 10^{-08} - j4.63 \times 10^{-10}$
2	$5.65 \times 10^{-14} - j1.18 \times 10^{-16}$	$2.66 \times 10^{-08} - j2.49 \times 10^{-10}$
3	$5.89 \times 10^{-14} - j2.98 \times 10^{-16}$	$2.68 \times 10^{-08} - j2.11 \times 10^{-10}$
4	$6.28 \times 10^{-14} - j7.05 \times 10^{-16}$	$2.69 \times 10^{-08} - j2.47 \times 10^{-10}$

Mathematically, a lossy inductor and a lossy capacitor can be defined, respectively, as

$$R + j\omega L = j\omega \left( L - j\frac{R}{\omega} \right) = j\omega L_{lossy}, \tag{15a}$$

$$G + j\omega C = j\omega \left( C - j\frac{G}{\omega} \right) = j\omega C_{lossy}. \tag{15b}$$

Since all the examples considered above have no substrate loss, only the inductive components of their PEEC models should be modified by adding the conductor loss of

$$R = \kappa \cdot \frac{l}{\sigma A}, \tag{16}$$

where  $\sigma$ ,  $l$ , and  $A$  are conductivity, length and cross-section area of the inductive mesh respectively. And  $\kappa$  ( $\leq 1$ ) is used to approximately account for the skin effect. In this case, the inductive components are now taking into account for both radiation loss and conductor loss. By setting  $\sigma$  to  $5.8 \times 10^7$  S/m and mesh thickness to  $1 \mu\text{m}$ , new component values of the concise models for the four antennas are obtained as shown in Tables 5 to 8. Comparing these values to those listed in Tables 1 to

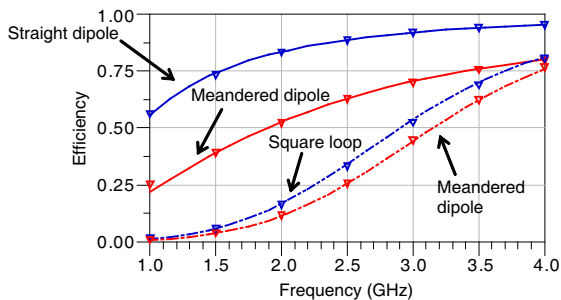


**Figure 9.** Estimated efficiencies of various electrically small antennas. Solid curves are results from a commercial full-wave MoM solver and triangular markers are results from the proposal method.

4, the radiation efficiency for these antennas can be calculated and are shown in Fig. 9. It is interesting to see that even though the meandered dipole has a larger radiating resistance than the straight one, it indeed is less efficient.

#### 4. DISCUSSION

In the above examples, the parameter  $\delta$  has been set to a large value such that all PEEC models were simplified to containing only the port nodes. These simplified circuits are indeed concise and reveal the most important features of the radiating structures being modeled, namely the radiation loss and net reactive energy. However, using a large value of  $\delta$  may produce an “oversimplified” circuit especially when  $ka$  is closer to 0.5. Notice that an “oversimplified” circuit is still numerically accurate in terms of the excitation port responses since there is no approximation made during the reduction process. However, some internal features of the radiating structure being modeled are hidden. Fig. 10 shows the derived concise circuits for the meandered dipole and square loop at 4 GHz with  $\delta$  being set to 0.15. Comparing with those shown in Fig. 7, the one for the dipole contains two extra (internal)

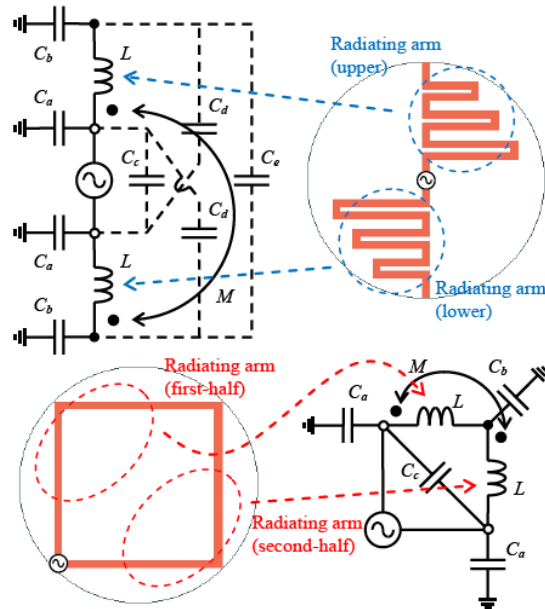


**Figure 10.** Concise equivalent circuits for the meandered dipole and square loop with  $\delta = 0.15$ .

**Table 9.** Component values.

	Meandered Dipole	Square Loop
$C_a$	$6.88 \times 10^{-14} - j3.62 \times 10^{-17}$ F	$7.66 \times 10^{-14} - j1.32 \times 10^{-17}$ F
$C_b$	$7.39 \times 10^{-14} + j2.49 \times 10^{-17}$ F	$1.46 \times 10^{-13} - j5.76 \times 10^{-17}$ F
$C_c$	$1.20 \times 10^{-14} - j2.07 \times 10^{-16}$ F	$1.91 \times 10^{-14} - j5.39 \times 10^{-16}$ F
$C_d$	$1.85 \times 10^{-14} - j2.81 \times 10^{-16}$ F	-
$C_e$	$8.34 \times 10^{-15} + j1.18 \times 10^{-16}$ F	-
$L$	$8.37 \times 10^{-09} - j1.03 \times 10^{-10}$ H	$1.05 \times 10^{-08} - j5.22 \times 10^{-10}$ H
$M$	$3.10 \times 10^{-10} - j1.06 \times 10^{-10}$ H	$-7.04 \times 10^{-11} + j4.68 \times 10^{-10}$ H

nodes whereas the one for the loop contains one extra (internal) nodes. These two circuits are definitely able to reveal the key internal features of the antennas. For instance, the two radiating arms and their associated inductances of each antenna are clearly represented by the two inductors in each circuit. Moreover, their self- and mutual capacitive couplings are represented by various capacitors as shown. Component values for these two cases are listed in Table 9.

## 5. CONCLUSION

An automatic MOR technique for generating a physical intuitive circuit model for electrically small radiating structures has been proposed in this paper. It is found out that the model is concise and contains all the key features of the structure being modeled. Specifically, the proposed algorithm can generate a very concise circuit model, which contains only the port nodes, so that the radiation loss can be represented by a single resistor. With this specific model, the radiation  $Q$  factor and efficiency of a radiating structure can be easily obtained. In addition, the conciseness of the reduced model can be controlled to reveal different levels of internal features for a given radiating structure. This capability is not available from typical commercial full-wave solvers. The MOR technique is particular useful for the design and analysis of integrated and electrically small antennas for modern wireless communication devices.

## ACKNOWLEDGMENT

This work was supported by University Grants Committee of Hong Kong under Grant AoE/P-04/08.

## REFERENCES

1. Ruehli, A. E., "Equivalent circuit models for three dimensional multiconductor systems," *IEEE Trans. Microwave Theory Tech.*, Vol. 22, 216–221, March 1974.
2. Heeb, H. H. and A. E. Ruehli, "Three-dimensional interconnect analysis using partial element equivalent circuits," *IEEE Trans. Circuits and Systems*, Vol. 39, 974–982, November 1992.
3. Kochetov, S. V., M. Leone, and G. Wollenberg, "PEEC formulation based on dyadic Green's functions for layered media in the time and frequency domains," *IEEE Trans. Electromagnetic Compatibility*, Vol. 50, 953–965, November 2008.
4. Jayabalan, J., B.-L. Ooi, M.-S. Leong, and M. K. Iyer, "Novel circuit model for three-dimensional geometries with multilayer dielectrics," *IEEE Trans. Microwave Theory Tech.*, Vol. 54, 1331–1339, June 2006.
5. Zhang, X. and Z. Feng, "A new retarded PEEC model for antenna," *IEEE 2008 Asia-Pacific Microwave Conf.*, Macau, 2008.
6. Sundberg, S. and J. Ekman, "PEEC modeling of antenna characteristics," *Proc. IEEE Int. Symp. EMC*, 580–585, Portland, 2006.
7. Yeung, L. K. and K.-L. Wu, "Generalized partial element equivalent circuit (PEEC) modeling with radiation effect," *IEEE Trans. Microwave Theory Tech.*, Vol. 59, 2377–2384, October 2011.
8. Balanis, C. A., *Antenna Theory: Analysis and Design*, John Wiley and Sons, New Jersey, 2005.
9. Antonini, G., D. Deschrijver, and T. Dhaene, "Broadband rational macromodeling based on the adaptive frequency sampling algorithm and the partial element equivalent circuit method," *IEEE Trans. Electromagnetic Compatibility*, Vol. 50, 128–137, February 2008.
10. Song, Z., D. Su, F. Duval, and A. Louis, "Model order reduction for PEEC modeling based on moment matching," *Progress In Electromagnetics Research*, Vol. 114, 285–299, 2011.
11. Wang, J. and K.-L. Wu, "A derived physically expressive circuit model for multilayer RF embedded passives," *IEEE Trans. Microwave Theory Tech.*, Vol. 54, 1961–1968, May 2006.